synergistic effect of ascorbate on the antioxidation activity of α-tocopherol.[30]

The redox potentials reported in Table IV were measured at high pH. Direct measurement in neutral or acid solutions is made impossible by the very low rates of electron transfer reactions involving the undissociated phenols.[13] Nevertheless, the values measured in the present work can be used to calculate the potentials in neutral and acid solutions if the $pK_a$ values of the compound and its radical are known. Such calculations for ascorbic acid and the three dihydroxybenzenes have been reported earlier.[13] Table V summarizes the redox potentials at pH 7 and 13.5 for several compounds for which the $pK_a$ values are known. In the case of TMPD, where both the compound and its radical do not undergo any acid-base equilibria between pH 7 and 13.5 and where the redox reaction studied does not involve any proton transfer, the potential is the same at both pH values. With all of the other compounds in Table V, the potential changes to an extent which depends on the $pK_a$ values, and as a result the relative oxidizabilities of the compounds change. For instance, at pH 13.5 ascorbate, hydroquinone, and catechol are much more easily oxidized than TMPD, whereas at pH 7 TMPD is the most powerful reductant in this group.

In conclusion, rapid one-electron transfer processes between various phenoxyl radicals and phenoxide ions, and the corresponding amino derivatives, have been observed by kinetic spectrophotometry. Analysis of the rates and equilibria led to the determination of one-electron oxidation potentials for the various compounds studied. Some of these compounds are of importance as antioxidants or as components of biological systems, possibly involved in electron transfer reactions. The knowledge of their redox potentials may help to achieve a better understanding of their function and may be useful in predicting redox potentials for similar compounds which are not easily accessible.

(30) Reference 3, p 207.

# Investigation of the Hydrolysis of Aqueous Solutions of Aluminum Chloride. 2. Nature and Structure by Small-Angle X-ray Scattering

**J. Y. Bottero,*† D. Tchoubar,‡ J. M. Cases,† and F. Flessinger§**

*Centre de Recherche sur la Valorisation des Minerais, L.A. no. 235 (CNRS), B.P. 40, 54501 Vandoeuvre-les-Nancy Cédex, France; Université d'Orléans, Laboratoire de Cristallographie, E.R.A. 841 (CNRS); Société Lyonnaise des Eaux et de l'Eclairage*

*(Received: March 31, 1981; In Final Form: January 11, 1982)*

The process of hydrolysis-precipitation of aluminum from aqueous aluminum chloride solution at 25 °C and for a concentration of $10^{-1}$ M has been studied by using solutions with a neutralization ratio $r = (NaOH)/(Al_T)$ equal to 2 and 2.5, by small-angle X-ray scattering using a synchrotron source. In the former case, the aluminum ion is embodied principally in a polymer with the formula $Al_{13}O_4(OH)_{28}^{3+}$ with an experimental radius of gyration of 9.8 Å, which corresponds to an ionic radius of 12.6 Å. In the second case, the aluminum is embodied partly in the species described above and partly in a colloidal species of chemical composition similar to that of the trihydroxide. The particle morphology of the colloidal species changes as a function of time. After aging for 1.5 h, the particles are cylindrical with a radius of about 15 Å and a length of 310 Å. After 24-h aging, the cylinders have agglomerated into more homogeneous platelets of diameter 500 Å and thickness 60 Å.

## Introduction

Aluminum chemistry is of considerable interest in geoscience and water treatment. Many authors have interpreted their results in terms of $Al^{3+}$ ion hydrolysis in acidic medium with the "core + links" theory.[1,2] This theory leads one to conceive, according to the neutralization ratio $r = (NaOH)/(Al_T)$, where the parentheses indicate the total sodium hydroxide and aluminum concentrations, a series of polymers the growth of which is bidimensional[3-9] and whose basic structure is a six-aluminum ring whose formula is $Al_6(OH)_{12}^{6+}$.

Some authors[1,3] suggest the existence of large, two-dimensional polymers able to contain more than 1000 atoms of aluminum. It appears that this growth model is not accepted by some authors[10] for systems such as chromia gels. According to these authors, growth along the C axis takes place immediately as a certain molecular weight is exceeded.

In an earlier publication,[11] we reported finding by $^{27}Al$ NMR and potentiometric titration five species in dilute solutions ($(Al_T) = 10^{-1}$ M) according to the neutralization ratio $r = (NaOH)/(Al_T)$: the monomers $Al(H_2O)_6^{3+}$, $Al(H_2O)_5(OH)^{2+}$, $Al(H_2O)_4(OH)_2^{+}$; a dimer $Al_2(OH)_2^{4+}$; a

† Centre de Recherche sur la Valorisation des Minerais.
‡ Université d'Orleans.
§ Société Lyonnaise des Eaux et de l'Eclairage.

(1) Sillen, L. G. *Acta Chem. Scand.* **1954**, *8* 299.
(2) Sillen, L. G. *Acta Chem. Scand.* **1960**, *15*, 1681.
(3) Hsu, P. H.; Bates, T. F. *Min. Mag.* **1964**, *33*, 749.
(4) Bersillon, J. L.; Hsu, P. H.; Fiessinger, F. *Soil Sci. Soc. Am. J.* **1980**, *44*, 630.
(5) Hem, J. D.; Roberson, C. E. *U.S. Geol. Surv. Water-Supply Paper* **1967**, *No. 1827 A.*
(6) Leonard, A. J.; Van Cauwelaert, F.; Fripiat, J. J. *J. Phys. Chem.* **1967**, *71*, 695.
(7) Vermeulen, E.; Geus, J. W.; Stol, R. J.; De Bruyn, P. L. *J. Colloid Interface Sci.* **1975**, *44*, 449.
(8) Stol, R. J.; Van Helden, A. K.; De Bruyn, P. L. *J. Colloid Interface Sci.* **1976**, *57*, 115.
(9) Matijevic, E.; Mathai, K. G.; Ottewill, R. H.; Kerker, M. *J. Phys. Chem.* **1961**, *65*, 826.
(10) Torralvo, F.; Alario-Franco, M. A. *J. Colloid Interface Sci.* **1980**, *77*, 1.
(11) Bottero, J. Y.; Cases, J. M.; Fiessinger, F.; Poirier, J. E. *J. Phys. Chem.* **1980**, *84*, 2933.

0022-3654/82/2086-3667$01.25/0 

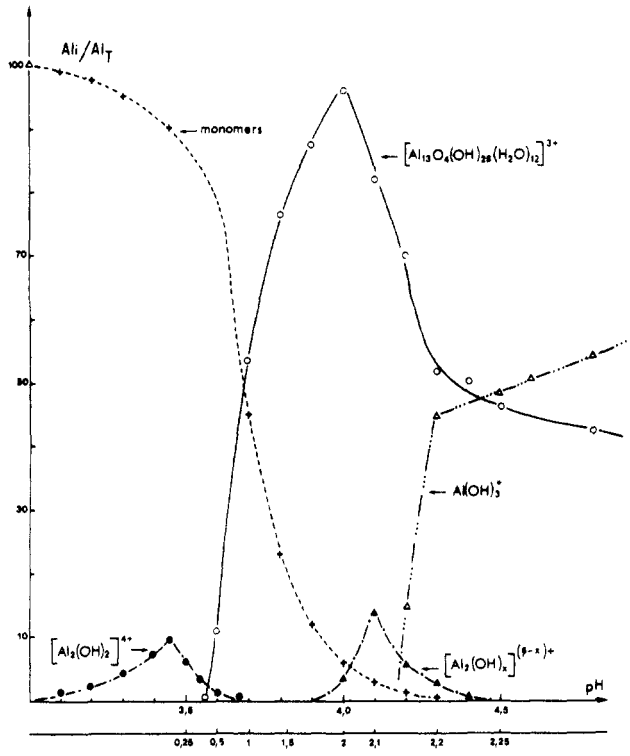


**Figure 1.** NMR and potentiometric titration results by Bottero et al. (1980).

three-dimensonal polymer with the formula $Al^{IV}O_4Al^{VI}_{12}(OH)_{28}^{3+}$, which will be designated $Al_{13}$, already described by Johansson[12] and Akitt.[14-16] This polymer has spherical symmetry. The octahedral aluminum atoms are equidistant from the central tetrahedral aluminum atom. And each octahedral aluminum atom is at equal distance from its neighbors. Also found was a charged nonsettlable colloidal gel (Figure 1). These species satisfy the following equilibrium equations:

$$Al^{3+} + H_2O \rightleftharpoons Al(OH)^{2+} + H^+ \qquad pK = 5.02^{13,17}$$

$$Al^{3+} + 2H_2O \rightleftharpoons Al(OH)_2^{+} + 2H^+ \qquad pK = 8.71^{18}$$

$$2Al^{3+} + 2H_2O \rightleftharpoons Al_2(OH)_2^{4+} + 2H^+ \qquad pK = 5.5^{11}$$

$$13Al^{3+} + 32H_2O \rightleftharpoons Al_{13} + 36H^+ \qquad pK = 105^{11}$$

$$Al^{3+} + 3H_2O \rightleftharpoons Al(OH)_3 + 3H^+ \qquad pK_S = 10.1^{11}$$

These results have been confirmed by recent work from highly diluted solutions: $10^{-2}$ and $10^{-3}$ M.[19]

In order to investigate particle shape and structure as well as the influence of aging, we have performed experiments using small-angle X-ray scattering. This experimental method has been used very little for studying solutions of aluminum. Rausch et al.[20] believe that they have identified the polymer $Al_{13}$ in concentrated solutions (1 M). Bale et al.[21,22] used gels at pH 7 and aluminum concentrations from 0.5 to 1 M and, by analogy with electron microscopy results, report the presence of platelet particles or homogeneous domains in the form of platelets. Our intention was precisely to avoid using electron microscope data which are unsuitable for studying gels and to interpret the scattering curves in their entirety (1) using Guinier's law at the lowest angles and, (2) using the Sturhman–Luzzati theory relative to dilute solutions.

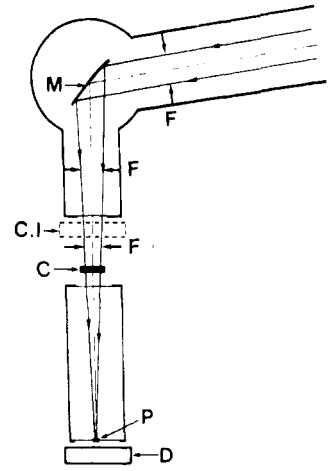


**Figure 2.** Experimental assembly: (F) antidiffusing slits, (M) monochromator, (CI) ionization chamber, (C) sample, (P) trap, (D) detector.

## Experimental Methods and Materials

*Beam Characteristics.* For this work, we made use of the synchrotron beam from the DCI storage ring at L. U.R.E. (University of Orsay); this source has particular advantages, in beam symmetry and energy, which make it possible to study weakly scattering systems in very short times: (1) The beam diverges very little in the vertical plan ($2 \times 10^{-3}$ rad). It is practical to obtain a point image of the source using a single-curve monochromator which focuses the beam in a horizontal plane, thus eliminating any instrumental deformation relating to the shape of the beam and its spectral content. (2) Since the beam is very intense, counting times are about 200 times shorter than when a conventional source is used.

*Characteristics of the Experimental Assembly.* The small-angle scattering assembly (Figure 2) includes a monochromator with variable curvature which is a germanium crystal and gives a convergent beam in the horizontal plane[23] with a wavelength resolution $\Delta\lambda/\lambda = 10^{-3}$. Spurious scattering (scattering due to the air, thermal scattering by the monochromator, and so on) is radically reduced by means of vacuum chambers and a series of antiscattering slits arranged along the beam path. The focal distance chosen was 2 m. At this distance the image of the beam is 800 $\mu$m wide in the horizontal plane and has a normal of 1 cm which can be reduced to 300 $\mu$m by a collimation. All of the components are movable on an optical bench. The sample-detector distance can be varied from a few centimeters to 1 m. We used a located detector of the LC-delay type, developed by E.M.B.L. (Hamburg) for use with synchrotron radiation.[24] This detector has

(12) Johansson, G. *Acta Chem. Scand.* **1960**, *14*, 771.
(13) Garrels, R. M.; Christ, C. L. "Equilibre des Minéraux et de Leurs Solutions Aqueuses": Gauthier-Villars: Paris, France, 1970.
(14) Akitt, J. W.; Greenwood, W. N.; Khandelwal, B. L. *J. Chem. Soc., Dalton Trans.* **1972**, 604.
(15) Akitt, J. W.; Greenwood, W. N.; Lester, S. D. *Chem. Commun.* **1969**, 988.
(16) Akitt, J. W.; Greenwood, W. N.; Lester, S. D. *J. Chem. Soc., Dalton Trans.* **1969**, 803.
(17) Robie, R. A.; Walbaum, D. R. *Geol. Surv. Bull. (U.S.)* **1968**, *No. 1259*.
(18) Parks, G. A. *Ann. Mines* **1972**, *57*, 1163.
(19) Bottero, J. Y.; Marchal, J. P.; Cases, J. M.; Fiessinger, F.; Poirier, J. E. *Bull. Soc. Chim. Fr.*, in press.
(20) Rausch, M. W.; Bale, H. D. *J. Chem. Phys.* **1964**, *40*, 11, 3391.
(21) Bale, H. D.; Schmidt, P. W. *J. Chem. Phys.* **1958**, *62*, 1179.
(22) Bale, H. D.; Schmidt, P. W. *J. Chem. Phys.* **1959**, *31*, 6.
(23) Tchoubar, D.; Rousseaux, F.; Pons, Ch.; Lemonier, M. *Nucl. Instrum. Methods* **1978**, *152*, 301.
(24) Gabriel, A.; Dalivergne, F.; Rosenbaum, G. *Nucl. Instrum. Methods* **1978**, *152*, 191.

the advantage of withstanding high fluxes without damage; its resolving power is 150 $\mu$m between two measuring points.

The range of the small angles investigated was obtained with the detector in the vertical position and a sample detector distance of 1 m. The Bragg zone analyzed was between 40 and 1000 Å. The wavelength used was 1.5 Å. As a result of the narrow beam, the only corrections necessary were those for absorption by the sample. In order to obtain the scattering due to the aluminum species, we subtracted the scattering by the solvent from the total, i.e., solutions of NaCl of suitable concentration determined by the neutralization ratio $r = (NaOH)/(Al_T)$.

*Specimens.* Three solutions were analyzed: with aluminum concentrations equal to $10^{-1}$ M and a neutralization ratio $r = 2$ (solution I) with nearly 100% of the aluminum embodied in the polymer $Al_{13}$; $r = 2.5$ (solution II), aged for 1.5 h with 28% of the aluminum embodied in the polymer $Al_{13}$ and 72% in colloidal particles; and, finally, $r = 2.5$ (solution III), aged for 24 h, i.e., with the solution in a state of "pseudoequilibrium" and 40% of the aluminum embodied in the polymer $Al_{13}$ and 60% in colloidal particles as described above.[11] The method of preparing these solutions was described in this earlier publication.

## Method of Interpretation

We shall apply the appropriate mathematical expressions to the diagrams recorded using the ponctual beam. It must be noted that the solutions investigated have a low concentration of $AlCl_3$: $10^{-1}$ M or 1.33% by weight of solid. Their viscosities at 25 °C are still close to that of water, and the maximum value is $1.25 \times 10^{-2}$ P for solution III. We shall therefore start from the assumption that the system is infinitely dilute, in other words, that the particles dispersed in the solvent do not interact. We shall also assume that we have a two-phase system: particles of uniform electron density and a solvent. It is then possible to analyze the small-angle scattering using a number of properties—enterely justified here—of a monodispersive or slightly dispersive system. We know in particular that, in the small-angle scattering curve, it is possible to consider three characteristic curves.[25]

(1) For the first, the innermost part of the scattering is sensitive to the size of the particles but not to their shape. In this part, the curve obeys the law of Guinier:

$$I(S) \simeq I(0) \exp\frac{4\pi^2 R_g^2}{3} S^2$$

where $I(S)$ is the scattered intensity, $S = \epsilon/\lambda$ where $\epsilon$ is the scattering angle and $\lambda$ the wavelength, $I(0)$ is the value at the origin of the intensity, and $R_g$ is the radius of gyration of the particle, which is determined, from the slope at the origin of the function $\ln I(S)$ vs. $S^2$. For a cylindrical particle of diameter $2R_c$ and thickness or height $2H_c$, we have

$$R_g^2 = R_c^2/2 + H_c^2/3 \tag{1}$$

For a spherical particle of radius $R$

$$R^2 = \tfrac{5}{3} R_g^2 \tag{1'}$$

This expression shows that $R_c$ and $H_c$ have approximately the same significance and that it is not absolutely possible to decide between an elongated cylinder or a platelet particle. Using Guinier's law, it is possible to extrapolate the scattering curve to $S = 0$ and hence to find $I(0)$. For a dilute and monodispersive system[25-27]

$$I(0) = K_1 V^2 (\Delta\rho_0)^2 \tag{2}$$

where $V$ = volume of the particle, and $\Delta\rho_0 = \rho_P - \rho_0$ with $\rho_P$ = average electron density of the particle and $\rho_0$ = average electron density of the solvent. $K_1$ is an absolute scale coefficient which depends on the incident beam intensity, the absorption in the specimen, and the number of scattering particles per unit surface area of the specimen. Using the initial assumptions and also assuming an ideally diluted solution of homogeneous and uniformly dispersive particles, it is also possible to use the total scattering power, $P(0)$, equal to the total contained of the scattering and given by the expression

$$P(0) = 4\pi \int_0^\infty S^2 I(S)\, dS = K_1 V (\Delta\rho_0)^2 \tag{3}$$

This parameter enables us to normalize all of the measured quantities to the scale of the particle. As an example, when expressions 2 and 3 are compared, the volume $V$ of the particle is determined from the ratio

$$I(0)/P(0) = V \tag{4}$$

regardless of the scale in which the specimen is analyzed.

(2) For the second part of the curve, the intermediate range of angles is sensitive to the shape of the particles. This part of the scattering curve has two characteristic properties. In the case of platelets of thickness $2H$ and radius $R$,[25] the scattering may be represented by the asymptotic function

$$I(S) \simeq I(0)/[S^2 \exp(-4\pi^2 S^2 H^2/3] \tag{5}$$

In the case of elongated cylinders of radius $R$ and height $2H$[25]

$$I(S) \simeq I(0)/[S \exp(-\pi^2 S^2 R^2)] \tag{6}$$

These two characteristic laws, if observed experimentally, may be associated with the first two properties and make it possible to determine particle size and shape.

(3) For the third part of the curve, the outermost part of the scattering depends on the surface area of the particles and, in the case of a colloidal suspension, on the surface area of the interface between particles and solvents. These properties are known as Porod's law and are related to the existence of a discontinuity in average electron density at the interface of the two media.[37] It is expressed in the following form: for large values of $S$, the characteristic product $S^4 I(S)$ tends to a constant limit defined by the expression

$$\lim 8\pi^3 S^4 I(S) = K_1 \sigma (\Delta\rho_0)^2 \tag{7}$$

where $\sigma$ is the surface area of the solute–solvent interface. By dividing eq 7 by eq 3, we obtain

$$\frac{\lim 8\pi^3 S^4 I(S)}{P(0)} = \frac{\sigma}{V} \tag{8}$$

The ratio $\sigma/V$ expresses the surface area of the particle in $m^2/cm^3$. The ratio $\sigma/V$ can also be expressed in terms of an average chord $\bar{l}$ where

$$\bar{l} = 4V/\sigma \tag{9}$$

The chord is defined as a straight line inside a particle bounded by the edges of the particle.[28,29] Generally

(25) Guinier, A.; Fournet, G. "Small-Angle X-ray Scattering"; Wiley: New York, 1955.

(26) Luzzati, V.; Tardieu, A.; Mateu, L. *J. Mol. Biol.* **1976**, *101*, 115.
(27) Sardet, C.; Tardieu, A.; Luzzati, V. *J. Mol. Biol.* **1976**, *105*, 383.

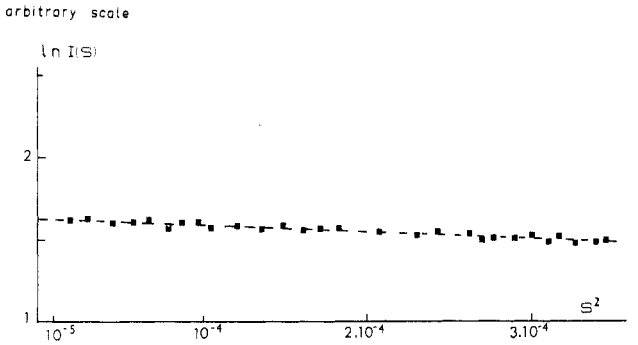


**Figure 3.** Scattering curve of the polymeric ion $Al_{13}$.

speaking, the particles vary in size and shape. The parameters given above then represent weighted means. The properties described above will be used in studying our specimens.

## Results and Discussion

*Investigation of Solution I (r = 2, Aged for 24 h).* Figure 3 shows that, in the angular domain studied, the curve of ln $I(S)$ against $S^2$ is a straight line. Equation 1 gives

$$\ln I(S) = \ln I(0) - (4\pi^2/3)R_g^2S^2$$

$$\rho = -0.97 \text{ (correlation coefficient)}$$

$$t = 100\% \text{ (confidence limits of correlation coefficient)}$$

i.e., $R_g = 9.8$ Å. Some NMR work[11] shows that this solution is almost entirely made up of $Al_{13}$ polymers. Since this polymer is of spherical shape,[11,12] the radius is then

$$R = (5/3)^{1/2}R_g = 12.6 \text{ Å}$$

The ionic radius of this polymer in the crystalline phase[12] is equal to 5.4 Å. Our results must be interpreted in terms of "hydrated" ions. It is well-known that in nonideal electrolytic solutions, the ions are surrounded by an ionic atmosphere, of a thickness depending on the ionic strength. In the present case, the ionic strength is equal to 0.6 M and is determined mainly by the $Na^+$ and $Cl^-$ ions. The $Cl^-$ ions are close to the polymer $Al_{13}$ and therefore play a substantial role in the small-angle scattering.

The surface area $\sigma/V$ determined from the experimental value of the radius $R = 12.6$ Å is $\sigma/V = 2380$ m$^2$/cm$^3$.

*Investigation of Solution II (r = 2.5, Aged for 1.5 h).* This solution is characterized by a turbidity which suggests the presence of fairly large scattering particles; another characteristic is a weak X-ray scattering power, owing to the fact that electron densities of the scattering particles and of the solvent are not very different. As a result, even using the synchrotron beam, the time taken to build up the small-angle scattering spectrum was still of the order of 2000 s. The use of NMR[11] shows that 72% of the aluminum is embodied in the colloidal species that are responsible for the turbid aspect. The plot of the scattered intensity in the plane (ln $I(S)$, $S^2$) (Figure 4A) shows an upturn at very small angles. In the region between $S = 8 \times 10^{-4}$ and $S = 1.18 \times 10^{-3}$, an apparent radius of gyration $R_g = 91$ Å is found. The characteristic product (Figure 5A) is constant and equal to $6.2 \times 10^{-6}$ over a relatively short range of angles and then subsequently rises again. This kind of curve is explicable by the fact that Porod's law is observed for the colloidal species but its range of observation is limited by the superimposition of scattering by the $Al_{13}$ polymers.

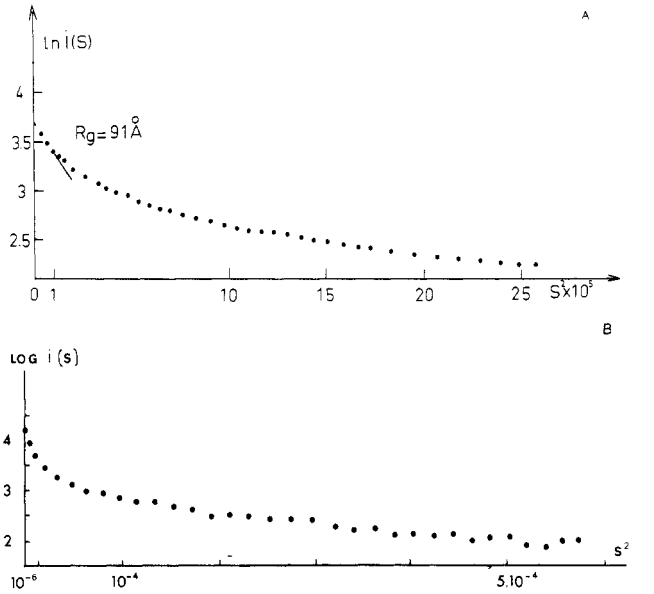


**Figure 4.** (A) Scattering curve of the species in the solution $r$ =; 2.5 aged for 1.5 h. (B) Scattering curve for the species contained in the solution $r = 2.5$ aged for 1.5 h.

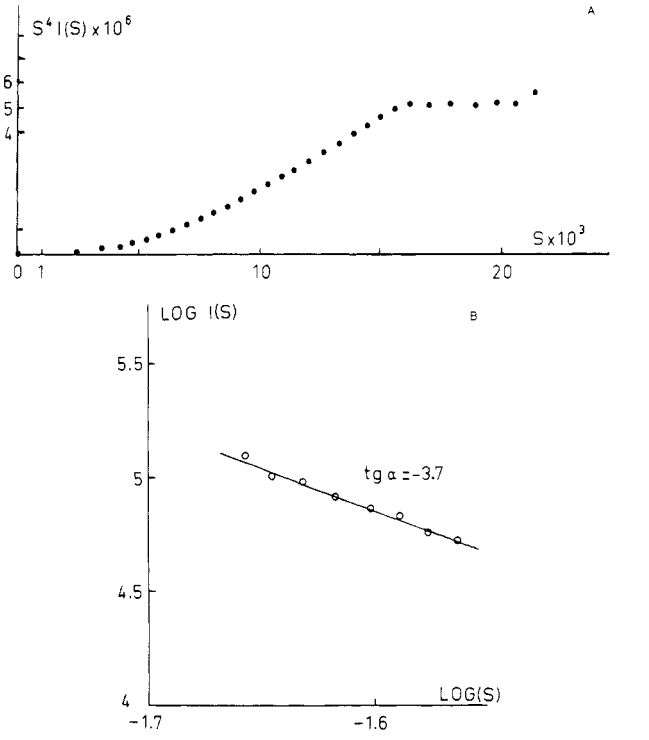


**Figure 5.** (A) Form and limit of the product $S^4I(S)$ for the species in the solution $r = 2.5$ aged for 1.5 h. (B) log $I(S)$ vs. log $S$ in the outer portion of the scattering of the solution $r = 2.5$ aged for 24 h.

Taking the Porod product to be constant at a value of $6.2 \times 10^{-6}$ for $S$ greater than or equal to $1.65 \times 10^{-2}$, one can determine $P(0)$, the total scattering power of the colloidal species (Figure 6A).

Applying relations 4, 6, and 7, we can then determine an apparent mean volume of these species, $V = 430250$ Å$^3$, an apparent surface area $\sigma/V$ approximately equal to 2000 m$^2$/cm$^3$, and an apparent mean chord $\bar{l}$ approximately equal to 20 Å. If these results are interpreted on the assumption that the colloidal species are isolated particles, approximately spherical in shape, the experimental values of the four parameters $R_g$, $V$, $\sigma$, and $\bar{l}$ are entirely incoherent (or are not correlated). In addition, the variation of the characteristic product (Figure 5A) before the hor-

(28) Mering, J.; Tchoubar, D. *J. Appl. Crystallogr.* **1969**, *2*, 128.
(29) Mering, J.; Tchoubar, D. *J. Appl. Crystallogr.* **1969**, *2*, 128.

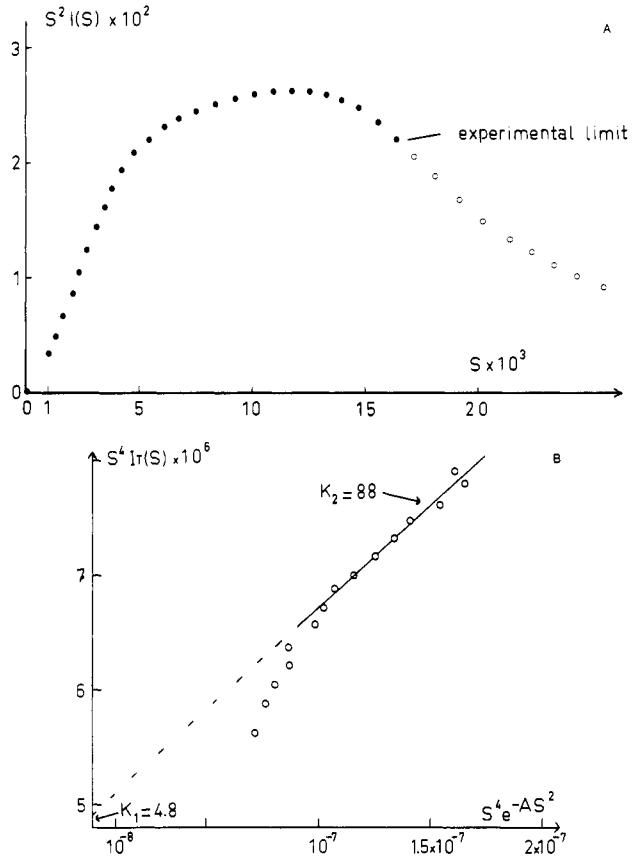


**Figure 6.** (A) Characteristic product relative to the solution $r = 2.5$ aged for 1.5 h. (B) $S^4I_T(S)$ vs. $S^4e^{-AS^2}$ curve in the outer portion of the scattering of the solution $r = 2.5$ aged for 24 h.

izontal platelet is also not characteristic of isolated, spherical particles. In this case, the curve should show a maximum at small angles.[28,29] On the other hand, a more reasonable hypothesis for representing these colloidal species seems to be a concept of aggregation of individual particles. The four parameters $R_g$, $V$, $\sigma$, and $\bar{l}$ can then be correlated if the colloidal particles of aluminum are considered to be isolated, highly anisotropic, and swollen by solvent. These colloidal particles could be made up of an aggregation of primary particle charges and linked together by $Cl^-$ ions from the solution or by hydrogen bonds. The values of $\sigma$ and $\bar{l}$ are then related to these primary domains while $V$ and $R_g$ characterize a mean volume and a mean radius of gyration for these aggregates, which are homogeneous. Supposing a cylindrical model for the aggregates, from the expression for the radius of gyration $R_g$ (eq 1′) and from the value of $V$

$$R_g^2 = R_c^2/2 + H_c^2/3$$

$$V = \pi(R_c^2)(2H_c)$$

giving a value for the height of the cylinder $2H_c = 310$ Å, and a radius of the transverse cross section $R_c$ is approximately 21 Å. Let us now look for the physical meaning of the parameters $\bar{l}$ and $\sigma$. The parameter $\bar{l}$ corresponding to the cylinder defined above is given by the relationship

$$\bar{l} = 2R_cH_c/(R_c + 2H_c)$$

or $\bar{l} = 39.3$ Å, a value which is twice that found experimentally. Two explanations are possible: (1) The cylindrical particles of height 310 Å and radius 21 Å are formed by the aggregation of elementary particles of aluminum hydroxide of the type $Al(OH)_X^{3-X+}$ separated from one another by a solvation layer formed by the water and the $Cl^-$ ions. In this case, the experimental values of $\sigma/V$ (2000

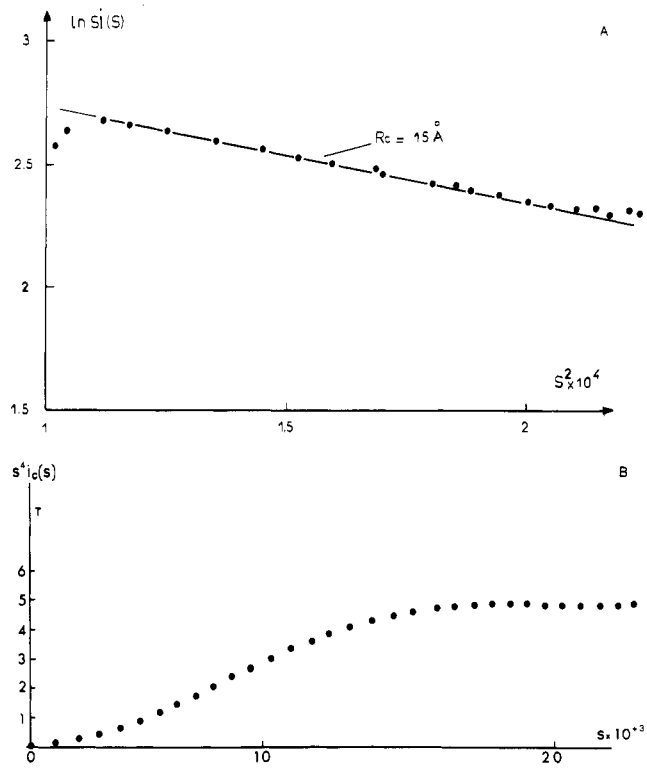


**Figure 7.** (A) Evolution of the function in $SI(S)$ vs. $S^2$. (B) Form and limit of the product $S^4I(S)$ for the aluminum colloidal species.

$m^2/cm^3$) and $\bar{l}$ (20 Å) correspond to these elementary, homogeneous domains. If these are spherically symmetrical, their radius is obtained from the relation[28,29] $\bar{l}_{exptl} = {}^4/_3R$, i.e., $R = 15$ Å. (2) It is also possible to conceive that these elementary domains are chains of length 310 Å with $\bar{l}$ being approximately equal to the diameter of their cross section. The radius of this chain will then be 10 Å.

It is thus clear that there is no unique solution to the problem. Experimental confirmation of the assumptions can be obtained by using relations 5 and 6. Only the asymptotic law for the elongated cylinders in Figure 7A, plotted in plane (log $[SI(S)/I(0)]$, $S^2$), shows a sufficiently long straight-line section, between $S^2 = 10^{-4}$ and $S^2 = 1.5 \times 10^{-4}$. The slope of the line gives a value for the radius of the transverse cross section, i.e., $R_c = 15$ Å.

This experimental value is of the same order of magnitude as the calculated values. It will be noted that these values for the radius of the elementary particles are not very different from that of the $Al_{13}$ polymers measured above. These colloidal aggregates can then be considered as micellae formed from the aggregation of elementary domains of homogeneous spheres with a radius close to 15 Å, jointed together in elongated cylinders of length 310 Å. These homogeneous spheres could be $Al_{13}$ polymers bound by their solvation sphere.

*Investigation of Solution III (Neuralization Ratio $r = (NaOH)/(Al_T) = 2.5$, Aged for 24 h).* After this period of aging, the solution contains 40% of the aluminum embodied in the $Al_{13}$ polymer and 60% in the colloidal gel,[11] which is responsible for the turbid aspect. We noted that the scattering power of the solution is appreciably higher than in the case of solution II. This increase in the scattering power reflects an increase in density contrast between the particles and the solvent. It also suggests that the scattering particles undergo densification as aging proceeds. The scattering curve (Figure 4B) plotted in the plane (ln $I(S)$, $S^2$) shows a substantial rise at very small angles which can be attributed either to highly anisotropic particles or to isolated spherical particles of widely varying

size. The slope of the curve at very small angles gives a radius of gyration $R_g$ = 140 Å. It was already observed for specimen II considered above that the scattering at larger angles by anisotropic particles is more specifically sensitive to their smaller dimension (diameter of a cylinder or thickness of a platelet). This property has been discussed by a number of workers.[21,22,30-33,36] However, we also observed that Porod's law applies only partially owing to the scattering by the small $Al_{13}$ polymers. Specimen III, aged for 24 h, contains an even higher proportion of isolated $Al_{13}$ polymers, which is the reason that the intensity $I(S)$ varies as $S^{-3.7}$ instead of as $S^{-4}$ for larger angle scattering (Figure 5B). It is then possible to separate the effects of the two types of scattering centers ($Al_{13}$ polymers and colloidal particles) because the total scattered intensity $I_T(S)$ may be expressed in the form

$$I_T(S) = I_p(S) + I_c(S) \quad (9)$$

where $I_p(S)$ is the intensity scattered by the $Al_{13}$ polymers and $I_c(S)$ is the intensity scattered by the particles of colloidal gel.

On the basis of the preceding discussion of the two specimens I and II, the outermost part of $I_c(S)$ must obey Porod's law while $I_p(S)$ for very small particles varies again according to Guinier's approximation. Thus, in the outermost scattering region where Porod's law applies, it is possible to express the total scattering by the following relation:

$$I_T(S) = K_1/S^4 + K_2 \exp(-AS^2) \quad (10)$$

$K_1$ will depend on the external surface area $\sigma$ of the colloidal particles or of the average chord $\bar{l}$. These two parameters are particularly sensitive to the smaller dimension of the particles. $K_2$ depends on the radius gyration of the polymers, with $A = (4\pi^2/3)R_g^2$. $K_1$ and $K_2$ also depend on the proportions of the two species that are present. The characteristic product of Porod can then be written

$$S^4 I_T(S) = K_1 + K_2 S^4 \exp(-AS^2) \quad (11)$$

The term $A$ is known from the examination of specimen I. Thus, by plotting the variation of the characteristic product against $S^4 \exp(-AS^2)$ (Figure 6B), it is possible to determine $K_1$ and $K_2$. In this way we can determine the scattering $I_c(S)$ for the colloidal particles only by applying relation 9. $I_p(S)$ is known from relations 10 and 11, and we can construct Porod's characteristic product (Figure 7B). By applying relation 4, it is possible to determine an average volume $V_c$ of the colloidal particles

$$I_c(0)/P_c(0) = 8.5 \times 10^6 \text{ Å}^3$$

where $P_c(0)$ is found by assuming that the Porod product remains constant for $S$ greater than or equal to $2.3 \times 10^{-2}$.

Relation 1 gives us the radius of gyration $R_g$ = 140 Å of these particles. The use of relations 5 and 6 raised the suggestion of scattering domains like platelets. In addition, this specimen seems more homogeneous than the preceding one and it was possible to compare the experimental

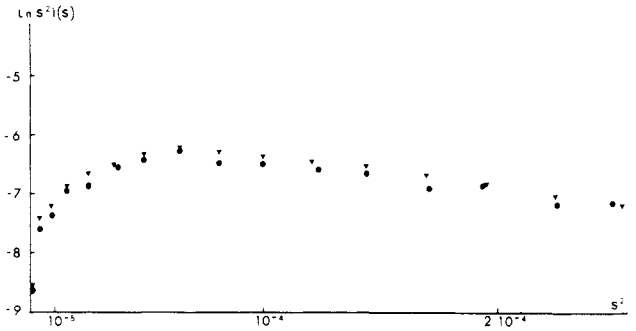


**Figure 8.** Comparison of the experimental and calculated characteristic functions brought back to the same scale: (●) experimental curve; (▼) calculated curve platelets with $2R$ = 500 Å and, $2H$ = 60 Å.

curve ln $S^2 I_c(S)$ with a calculated curve ln $S^2 i(S)$ where $i(S)$ is the intensity scattered by a homogeneous platelet of radius $2R$ and thickness $2H$.[25]

$$i(S) = \int_0^{\pi/2} \frac{\sin^2(2\pi SH\cos\theta)}{(2\pi SH\cos\theta)^2} \frac{4J_1^2(2\pi SR\sin\theta)}{(2\pi SR\sin\theta)^2} \sin\theta\, d\theta \quad (12)$$

where $\theta$ is the angle between the vector $\vec{S}$ and the axis of the platelet. $J_1$ is a Bessel function of the first kind and order 1.

Figure 8 shows that an acceptable superposition of two curves is obtained for a homogeneous platelet with $2R_c$ = 500 Å and $2H_c$ = 60 Å. By comparing the experimental curve ln $S^2 I(S)$ with a theoretical curve, it is possible to work out an average dimension for the platelets and an average radius of gyration calculated by using the relation[25]

$$R_g^2 = \frac{R_c^2}{2} + \frac{H_c^2}{3} = \frac{(250)^2}{2} + \frac{(30)^2}{3}$$

i.e., $R_g$ = 180 Å. The experimental radius of gyration is only 140 Å. One possible explanation for this difference is an electronic heterogeneity of the particles of colloidal gel which reduces the value of the radius of gyration.[26,27] The average volume $V_c$ obtained by relation 4 is lower than the theoretical volume $V$ for a homogeneous platelet:

$$V_{Th} = (\pi R^2)(2H) = 1.18 \times 10^7 \text{ Å}^3$$

where $V_{Th}$ is the theoretical volume calculated for a homogeneous platelet. The difference between the two values may be explicable by an electronic heterogeneity in the particles of colloidal gel.

Finally, the experimental values for the surface area and for the average chord $\bar{l}$ obtained by using eq 6 are

$$S_{Sp} = 0.16 \text{ Å}^2/\text{Å}^3 \text{ or } 1600 \text{ m}^2/\text{cm}^3$$

$$\bar{l}_{exptl} = 4P(0)/[\lim 8\pi^3 S^4 I_c(S)] = 25\text{Å}$$

If the particles were homogeneous we should have $\bar{l} = (2R_c)(2H_c)/(I_c + 2H_c)$ = 97 Å, a value which corresponds to a surface area of about 400 $m^2/cm^3$, while experiments give the value $\bar{l}$ = 25 Å. As for specimen II, it is possible to conclude that this particle has an internal surface created by the aggregation of elementary homogeneous domains leading to a characteristic Porod product (Figure 7B) simiilar to that obtained for specimen II. This structure is feasible on the assumption that the cylindrical particles swollen with solvent observed in specimen II undergo densification due to internal reorganization and thus reject a substantial part of the $Cl^-$ ions into the solvent as they are converted into relatively homogeneous cylinders. The average chord $\bar{l}$ which was theoretically of the

(30) Fedorova, I. S.; Emel'Yanov, V. B. *J. Colloid Interface Sci.* **1977**, *59*, 106.
(31) Schmidt, P. W.; Emel'Yanov, V. B.; Fedorava, I. S. *J. Colloid Interface Sci.* **1978**, *67*, 226.
(32) Kratky, O.; Porod, G.; Sekora, A.; Paletta, B. *J. Polym. Sci.* **1955**, *16*, 163.
(33) Kratky, O.; Miholic, G. *J. Polym. Sci.* **1963**, *2*, 449.
(34) Shoen, R.; Roberson, C. E. *Am. Mineral.* **1970**, *55*, 43.
(35) Hurbain-Faucon, A. Thèse Doctorat, Montpellier, France, 1966.
(36) Pringle, O. A.; Schmidt, P. W. *J Colloid Interface Sci.* **1977**, *60*, 2, 252.
(37) Pons, Ch. H. Thèse Doctorat d'Etat, France, 1980.
(38) Sadoc, J. F. *J. Non-Cryst. Solids* **1981**, *44*, 1.

order of 39 Å is equal now to 25 Å as a result of this densification. In specimen III, aged for 24 h, we therefore observe the association of these homogeneous cylindrical domains into heterogeneous platelets. The $Cl^-$ ions in the solution are still able to penetrate inside these platelets, for example, along the homogeneous cylindrical domains.

## Conclusion

An X-ray scattering investigation of solutions of aluminum chloride in a state of pseudoequilibrium, containing a polymeric, spherical ion with formula $Al_{13}O_4(OH)_{28}(H_2O)_8^{3+}$ (solution $r = 2$)[11] or a mixture of $Al_{13}$ polymers and particles of a colloidal gel (solutions II and III), $r = 2.5$, aged for 1.5 and 24 h, indicates certain structural features of these colloidal gels and a number of important aspects of their aging process.

Investigation of solution I ($r = 2$) containing 90% of aluminum embodied in the $Al_{13}$ polymer gave an average measured radius of 12.6 Å. This value demonstrates that the solvation layer of the polymers has substantial thickness. This polymer has an icosahedral structure; the tetrahedral central aluminum is very symmetrically surrounded by 12 octahedral aluminum.

In solution II ($r = 2.5$, aged 1.5 h), the small-angle X-ray scattering shows particles of gel that are highly heterogeneous owing to their being swollen by solvent. It is possible to characterize these particles of gel—which probably vary widely in size—by an average cylindrical particle model 310 Å long and 30 Å in diameter. These particles are formed from homogeneous spherical particles agglomerated by water molecules and $Cl^-$ ions of solvation. It is obvious that these homogeneous particles are $Al_{13}$ polymers which are in part released in the solution following rupture of intermolecular bonds during aging. The experimental value of the surface area of 2000 $m^2/cm^3$ is related to the elementary homogeneous spherical particle of $Al_{13}$.

For solution III, with $r = 2.5$, aged for 24 h, the small-angle scattering shows a densification of the particles of colloidal gel through an increase in the difference of electron density between the particles and the solvent. The observed particles are much more uniform in size and shape than those in specimen II and appear in the form of platelets with an average thickness of 60 Å and an average diameter of 500 Å. These particles retain a total surface area of about 1600 $m^2/cm^3$, which may be interpreted as being due to a further agglomeration of the cylindrical masses mentioned above, which have undergone a reorganization, rejecting a proportion of the $Cl^-$ ions related to their solvation layer into the solvent.[35] Certainly the icosahedral structure of the polymers is destroyed, and the central tetrahedral is distorted.[38] An aging process of this kind, demonstrated by a direct—i.e., nondestructive—experiment, is the first stage in the formation of gibbsite in an acidic medium. A systematic study is being made of the successive stages of reorganization. We consider that the interest of this work is to show the importance of the icosahedral structure of the $Al_{13}$ polymer in the germination of trihydroxides. There is structural continuity between the $Al_{13}$ polymers, the gel aged for 1.5 h, and the gel aged for 24 h, reflected by a relative conservation of the surface area of the different systems.

*Acknowledgment.* We express our sincere gratitude for technical assistance from the L.U.R.E. and the linear accelerator staff at the University of Orsay.

# Laser-Excited Infrared Fluorescence in Oxalyl Fluoride. Relaxation in the Presence of a Low-Energy, One-Dimensional Quasicontinuum

**Toomas H. Allik and George W. Flynn***

*Department of Chemistry and Columbia Radiation Laboratory, Columbia University, New York, New York 10027*
*(Received: January 27, 1982; In Final Form: April 19, 1982)*

Fluorescence has been observed from various fundamental and combination states of oxalyl fluoride excited by a Q-switched $CO_2$ laser. The presence of a low-frequency torsional mode in this molecule provides a one-dimensional quasicontinuum of vibrational levels at energies above the barrier to rotation about the C–C bond. Intermode vibrational relaxation rates in $(COF)_2$ are extremely rapid (possibly collisionless). The observed temperature dependence of fluorescence intensity and the overall rapid equilibration in $(COF)_2$ suggest a mechanism in which many rovibrational transitions that possess $\nu_{10}$ character (e.g., $0 \rightarrow \nu_{10}$, $\nu_{10} \rightarrow 2\nu_{10}$, $\nu_x \rightarrow \nu_x + \nu_{10}$, etc.) are excited by the laser.

## Introduction

Time-resolved, laser-excited fluorescence experiments have been employed for some time to study vibrational relaxation in simple rigid polyatomic molecules. A great deal of information concerning vibration-to-vibration (V–V) and vibration to translation/rotation (V–T/R) energy transfer processes in molecules such as $CH_4$,[1] $CH_3F$,[2] OCS,[3] ONF,[4] and $SO_2$[5] has been obtained in this way. Kinetic maps for these molecules have been determined under weak laser excitation where the excited-state population can relax through collisions to its equilibrium value via a unique or nearly unique kinetic pathway. Although a variety of energy transfer pathways do exist in many molecules, most of them are unimportant either for dynamical reasons or because many energy levels never ac-

(1) J. T. Yardley and C. B. Moore, *J. Chem. Phys.*, **45**, 1066 (1966); **49**, 1111 (1968).
(2) (a) R. S. Sheorey, R. C. Slater, and G. W. Flynn, *J. Chem. Phys.*, **68**, 1058 (1978); (b) R. S. Sheorey and G. W. Flynn, *ibid.*, **72**, 1175 (1980).
(3) M. L. Mandich and G. W. Flynn, *J. Chem. Phys.*, **73**, 1265 (1980).
(4) R. Kadibelban, W. Janiesch, and P. Hess, *Chem. Phys.*, **60**, 215 (1981).
(5) D. Siebert and G. Flynn, *J. Chem. Phys.*, **62**, 1212 (1975).

0022-3654/82/2086-3673$01.25/0 